Chemical Engineering Journal 356 (2019) 904–914

Contents lists available at ScienceDirect

Chemical Engineering Journal

journal homepage: www.elsevier.com/locate/cej

Peroxymonosulfate activation for efficient sulfamethoxazole degradation by Fe_3O_4/β-FeOOH nanocomposites: Coexistence of radical and non-radical reactions

Chenxu Li[a], Jiaen Wu[b], Wei Peng[a], Zhendong Fang[a,*], Jie Liu[a,*]

[a] Department of Military Facilities, Army Logistics University, Chongqing 401311, China
[b] Department of Chemical Engineering and Chemistry, Eindhoven University of Technology, De Lismortel 42 316, 5612 AR Eindhoven, The Netherlands

HIGHLIGHTS

- Fe_3O_4/β-FeOOH nanocomposites was prepared and characterized.
- The SMX degradation can be achieved by the Fe_3O_4/β-FeOOH/PMS.
- Both sulfate radical and singlet oxygen are the dominant radicals to SMX degradation.
- The tunnel-type structure and surface oxygen vacancies of β-FeOOH can active PMS.

GRAPHICAL ABSTRACT

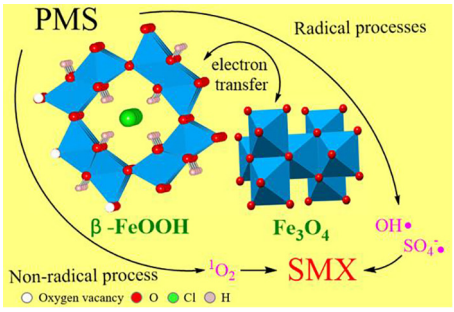

ARTICLE INFO

Keywords:
Fe_3O_4/β-FeOOH nanocomposites
Sulfamethoxazole
Peroxymonosulfate
Sulfate radicals
Singlet oxygen

ABSTRACT

Environmental friendly magnetic Fe_3O_4/β-FeOOH nanocomposites with low cost were prepared via a simple one pot method and their physiochemical properties were investigated. The Fe_3O_4/β-FeOOH nanocomposites efficiently catalyzed the activation of peroxymonosulfate (PMS) for sulfamethoxazole (SMX) degradation and can be easily recovered through magnetic separation. The effects of catalyst dosage, PMS dosage, temperature and pH were evaluated. The catalyst showed great stability and reusability based on the successive degradation cycles. The reactive oxygen species (ROS) including sulfate radical ($SO_4^{-\cdot}$), hydroxyl radical (·OH) and singlet oxygen ($^1O_2$) were generated in the Fe_3O_4/β-FeOOH/PMS system, while both of $SO_4^{-\cdot}$ and $^1O_2$ were dominantly attributed to the SMX degradation. The special tunnel-type structure and surface oxygen vacancies of β-FeOOH may be responsible for the high catalytic activity towards PMS to degrade SMX. At last, the catalytic mechanism of PMS on the surface of catalysts were proposed.

1. Introduction

Since 1970, the worldwide usage of antibiotics has caused an alarming concern for their hazards to the environment and public health [1,2]. Antibiotics have been widely used in the prevention and therapy of human diseases. As one of the most important sulfonamide antibiotics, sulfamethoxazole (SMX) is often detected in wastewater and may cause antibiotic pollution problems [3,4]. However, owing to the good chemical stability and poor biodegrability of refractory organic pollutants [5,6], effective removal of antibioticslike SMX is a big challenge to traditional wastewater treatment processes.

Advanced oxidation process (AOP) is an effective method for

* Corresponding authors.
E-mail addresses: fangzhendong@hotmail.com (Z. Fang), liujiely@hotmail.com (J. Liu).

https://doi.org/10.1016/j.cej.2018.09.064
Received 8 April 2018; Received in revised form 5 September 2018; Accepted 8 September 2018
Available online 08 September 2018
1385-8947/

mineralizing refractory organic contaminants due to the reactive oxygen species (ROS) generated from activation of oxidants [7,8]. The advanced oxidation technology based on peroxymonosulfate (PMS) activation is developed to degrade refractory organic pollutants in wastewater. Generally, $SO_4^{-\cdot}$ are considered as the dominant radical species attribute to the organic pollutants degradation. Compared with ·OH (1.8–2.7 V) [9], $SO_4^{-\cdot}$ (2.5–3.1 V) features its higher redox potential under neutral conditions and longer half-life (30 ~ 40 μs vs 20 ns) [10]. In addition, pollutants degradation via a non-radical oxidation process by generating $^1O_2$ is put forward in some studies [11,12].

PMS activated by transition metal ions is an effective method to produce sulfate radicals [13]. Among the various activation methods of PMS, potentially carcinogenic Co(II) ion owned the best catalytic activity [14]. At present, heterogeneous catalysis of PMS is developed to replace conventional homogeneous catalysis reaction because of its advantages such as low environmental pollution, low dosage and reusability of catalyst. Though heterogeneous Co-bearing catalysts can activate PMS efficiently [15–17], the leaching of toxic Co(II) is still inevitable.

Iron-based catalysts, with the characteristics of huge abundance and environmental friendly, are important transition metal materials to replace Co-catalyst. In the previous study, Fe^0@CS [18], Fe@ACFs [19], $CuFe_2O_4$ [20] and $CuFeO_2$ [21] have been synthesized and exhibited excellent performance in activation of PMS. However, the complicated preparation method and high synthesis temperature may confine their further applications.

As an environmental friendly material, FeOOH has been studied in heterogeneous Fenton-like reaction [22–24], while little has been known about its reaction with PMS so far. On the other hand, FeOOH is usually separated from reaction system by centrifugation or filtration, which makes separation and recycle of the catalyst difficult. Fe_3O_4 could be easily collected from liquid by magnetic separation, and the leaching iron ion from Fe_3O_4 can react with PMS. Nie et al. synthesized Cu^0-Fe_3O_4 composites for PMS activation to degrade RhB. The results showed that the degradation of RhB with Cu^0-Fe_3O_4 was about four times greater than that with Fe3O4 particles [25]. Mohammad et al. used Fe_3O_4-TiO_2 as photocatalyst to degrade Brilliant Blue FCF (BBF) with PMS and found that Fe_3O_4–TiO_2 had the best photocatalytic activity compared with Fe_3O_4 and TiO_2. In addition, Fe_3O_4-TiO_2 could be separated with magnet [26]. Liu et al. synthesized magnetic Fe_3O_4-MnO_2 core-shell nanocomposites to activate PMS for 4-chlorophenol degradation and demonstrated the synergistic mechanism between Fe_3O_4 and MnO_2 [7]. Therefore, hybrid materials containing FeOOH and Fe_3O_4 may have great potential for PMS activation.

In this study, a novel PMS activator, magnetic Fe_3O_4/β-FeOOH nanocomposites were prepared via a simple one pot method to activate PMS for SMX degradation, the catalytic performance and PMS activation mechanism was investigated. As far as we know, for the first time, Fe_3O_4/β-FeOOH nanocomposites were used for catalytic activation of PMS to degrade SMX degradation.

2. Materials and methods

2.1. Chemicals

Ferrous chloride ($FeCl_2$) and ferric chloride ($FeCl_3{\cdot}6H_2O$) were provided by Macklin Reagent Co., Ltd (Shanghai, China). sodium sulfite (Na_2SO_3), Sodium hydroxide (NaOH), ethanol and *tert*-butyl alcohol (TBA) were purchased from Xilong Chemical Co., Ltd (Shantou, China). Polyvinylpyrrolidone (PVP, K-30), sulfamethoxazole (SMX), peroxymonosulfate ($2KHSO_5{\cdot}KHSO_4{\cdot}K_2SO_4$) and furfuryl alcohol (FFA) were obtained from J&K Scientific Ltd (Beijing, China). All the chemical reagents were used directly as we received.

2.2. Preparation of catalysts

2.2.1. Preparation of Fe_3O_4/β-FeOOH

Fe3O4/β-FeOOH was one-pot synthesized by means of hydrothermal method. In brief, PVP (1.5 g), $FeCl_3{\cdot}6H_2O$ (5.4 g) and $FeCl_2$ (1.0 g) were dissolved in 200 mL deionized water followed by ultrasonic treatment for 5 min and further with continuous gentle stirring for 1 h at 353 K. And then, 2.0 M NaOH was dripped into the mixture until the pH value reached 6. The production was aged for 2 h and cooled down naturally. At last, the powder was collected through magnetic separation and washed repetitively with deionized water and anhydrous ethanol, the Fe3O4/β-FeOOH nanocomposites were obtained after drying at 323 K overnight.

2.2.2. Preparation of Fe_3O_4

20 mL of 2.0 M NaOH was dripped into 200 mL deionized water containing $FeCl_3{\cdot}6H_2O$ (2.7 g), $FeCl_2$ (1.0 g) and PVP (1.5 g) with stirring. The black precipitate was aged for 3 h under 343 K. The solids were gathered with magnetic separation and repetitively washed with deionized water and anhydrous ethanol, the Fe3O4 nanoparticles were obtained after drying at 323 K overnight.

2.2.3. Preparation of β-FeOOH

PVP (1.5 g) and $FeCl_3{\cdot}6H_2O$ (2.7 g) were dissolved in 200 mL deionized water followed by continuous gentle stirring for 3 h at 353 K. The orange-yellow powders were collected by centrifugal separation and repetitively washed with deionized water and anhydrous ethanol, the β-FeOOH nanoparticles were obtained after drying at 323 K overnight.

2.3. Characterization of catalysts

X-ray diffractomer (XRD, Rigaku D/MAX-2000), vibrating sample magnetometer (VSM, JDM-13), X-ray photoelectron spectroscopy (XPS, ESCALAB250Xi), Fourier infrared spectroscopy (FT-IR, Thermo Electron), Micromeritics ASAP 2020 automated system (Quantachrome, US, performed at 77 K) and transmission electron microscope (TEM, FEI F20) was used to determine the properties of the resultant samples.

2.4. Degradation of SMX

The degradation reactions were carried out in 250 mL conical flask. In a typical experiment, 0.02 g catalyst was well dispersed in 100 mL 5 mg/L of SMX solution, the mixture was mechanically stirred at 293 K for 30 min in the darkness. Later, 0.15 g/L PMS was added to the solution. At designated time intervals, 1.0 mL solution samples were taken and immediately filtered to remove the catalyst, followed by adding 20 μL of 1 M Na_2SO_3 to quench PMS. Sodium tetraborate buffer was used to stabilize the pH value. The concentration of SMX was detected by high-performance liquid chromatograph (HPLC). In operating parameters experiments, only one parameter changed each time while the others remained the same as in the typical experiment. In quenching experiments, the quenching agents were added to the solution earlier than PMS. For the recycle runs of SMX degradation, the used catalyst was collected by magnetic separation after the degradation experiments and washed with deionized water three times before the next test run. Afterwards, the catalyst was dispersed in 100 mL solution containing the same concentration of Oxone and SMX. All experiments were repeated three times, and the results were average of the three sets of data with a relative standard deviation less than 5%. The leaching Fe^{3+} was directly detected by Inductively coupled plasma atomic emission spectroscopy (ICP-AES).

2.5. Chemical analysis

A HPLC (Agilent 1260 Infinity II) with a UV detector at a wavelength of 260 nm was employed to detected the concentration of SMX.

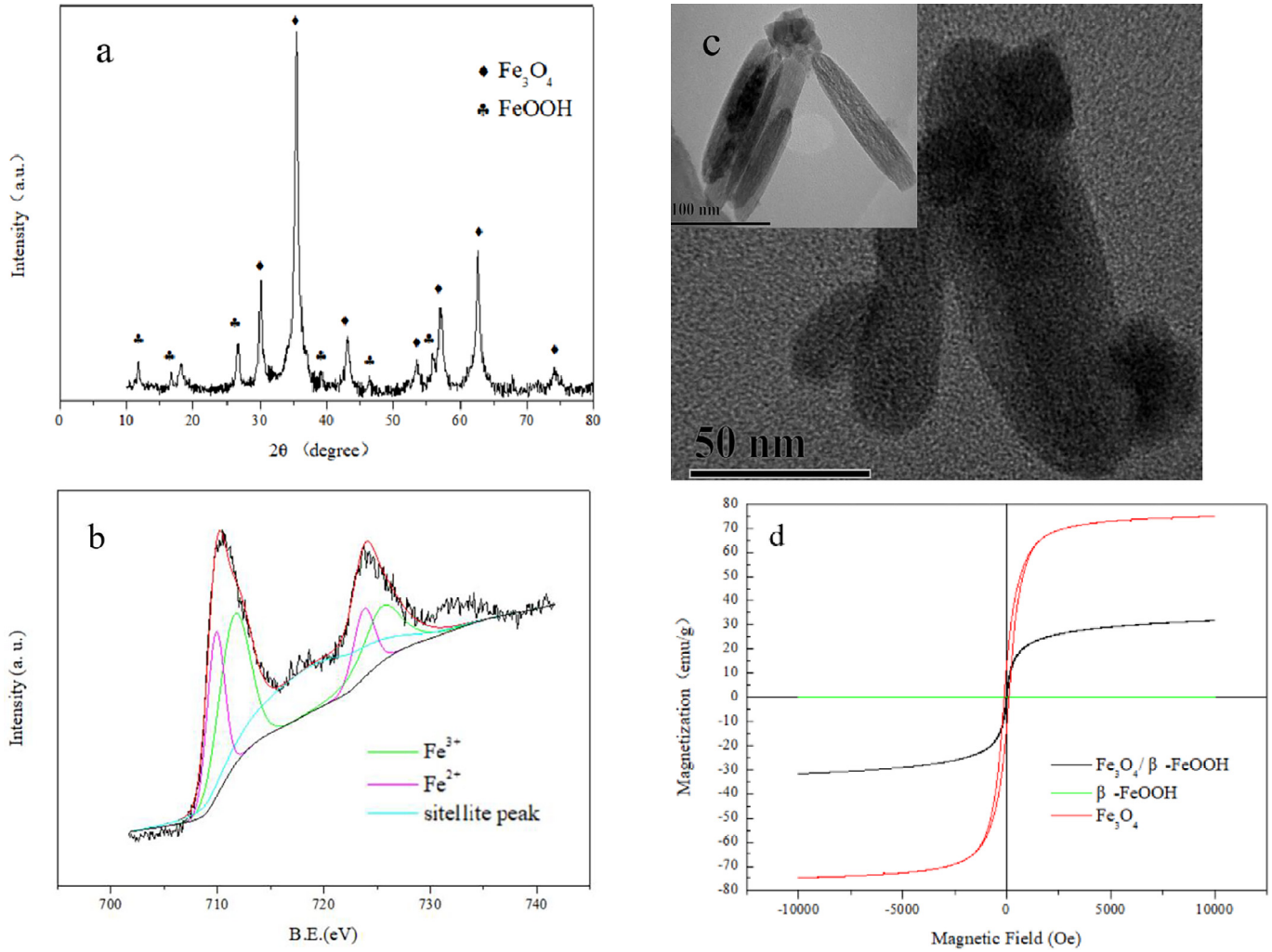

Fig. 1. (a) XRD pattern, (b) XPS Fe 2p survey, (c) TEM images and (d) Magnetization curve of Fe_3O_4/β-FeOOH magnetic nanoparticles.

The mobile phase composed of 40% methanol and 60% ultrapure water was acidified by 0.1% glacial acetic acid with the flow rate of 1.0 mL/min. The oven temperature was controlled at 40 °C and the injection volume was 20 μL. The pH of solution was determined with a pH meter (HQ40d, Hach, USA). The Fe ion leaching was monitored by ICP-MS (Agilent 7500, USA). In addition, a FA200 ESR spectrometer was used for electron spin resonance (ESR) analysis, 5,5-Dimethyl-1-pyrroline N-oxide (DMPO) and 2,2,6,6-Tetramethyl-4-piperidinol (TMP) were chosen as spin-trapping reagent for $SO_4^{\cdot-}$, ·OH and $^1O_2$.

3. Results and discussion

3.1. Characterization of Fe_3O_4/β-FeOOH

The result of XRD (Fig. 1a) showed that all diffraction peaks of synthesized solids meet excellent with the standard data for face-centered cubic crystal of Fe_3O_4 (JCPDS no. 79–0417, a = b = c = 8.394 Å) [7] and tetragonal β-FeOOH (JCPDS no. 80–1770, a = 10.54 Å and c = 3.03 Å) [27], indicating that the obtained samples were two-component mixtures of Fe_3O_4 and β-FeOOH. XPS was used to further analyzed the composition and valence state of elements in the surface of the samples. As shown in Fig. 1b, Fe^{2+} and Fe^{3+} were identified since 710.06 eV, 723.96 eV for Fe^{2+}, 711.60 eV and 725.50 eV for Fe^{3+} with a shake-up satellite at 718.83 eV [28,29]. In comparison with the XPS spectra of Fe_3O_4 (Fig. S1a) and β-FeOOH (Fig. S1b), the ratio of Fe^{2+} in the composites was higher than β-FeOOH and lower than Fe_3O_4.

Fig. 1. (*continued*)

The FTIR spectrum for the Fe_3O_4, β-FeOOH and the composites were exhibited in Fig. S2. The strong absorption band around 3403 cm^{-1} was ascribed to the stretching of O–H in β-FeOOH [30]. The typical low frequency band at around 578 cm^{-1} of β-FeOOH and Fe_3O_4 sample referred to Fe^{III}-O vibration in octahedral and tetrahedral sites and that 438 cm^{-1} in Fe_3O_4 sample was ascribed to Fe^{II}-O vibration in octahedral sites [31,32]. Besides, the band at 578 cm^{-1} of β-FeOOH in the composites had a red-shift to 611 cm^{-1}, which confirmed the successful combination of β-FeOOH and Fe_3O_4 [33].

The morphology and the particle size of pure β-FeOOH and Fe_3O_4/β-FeOOH nanoparticles were investigated by TEM (Fig. 1c). TEM images showed that all β-FeOOH crystals were in spindle-shaped, the small cubic crystals of Fe_3O_4 were decorated on spindle-shaped β-FeOOH, the lengths and the widths of β-FeOOH were 110–200 nm and 33 to 43 nm, respectively. The magnetization characters of samples at 300 K were shown in Fig. 1d. Obviously, Fe_3O_4/β-FeOOH had a specific magnetization (Ms) value of 31.41 emu g^{-1} at 9.5 kOe. It was indicated that the nanoparticles possessed a typical weak ferromagnetic property and could be easily separated from the treated water, which is also helpful for recycling. The N_2 adsorption/desorption isotherms and the associated pore distributionwere shown in Fig. S3. It can be seen that all the samples belonged to type IV isotherm with H3 type hysteresis loops. The surface areas of Fe_3O_4, β-FeOOH and Fe_3O_4/β-FeOOH were 88.77 m^2/g, 133.63 m^2/g and 111.91 m^2/g, respectively. The Fe_3O_4/β-FeOOH had larger specific surface area than Fe_3O_4 MNPs (86.55 m^2/g) [34] and Fe_2O_3 nanoparticles (24.76 m^2/g) [35]. Based on the results, Fe_3O_4/β-FeOOH magnetic nanoparticles were successfully synthesized

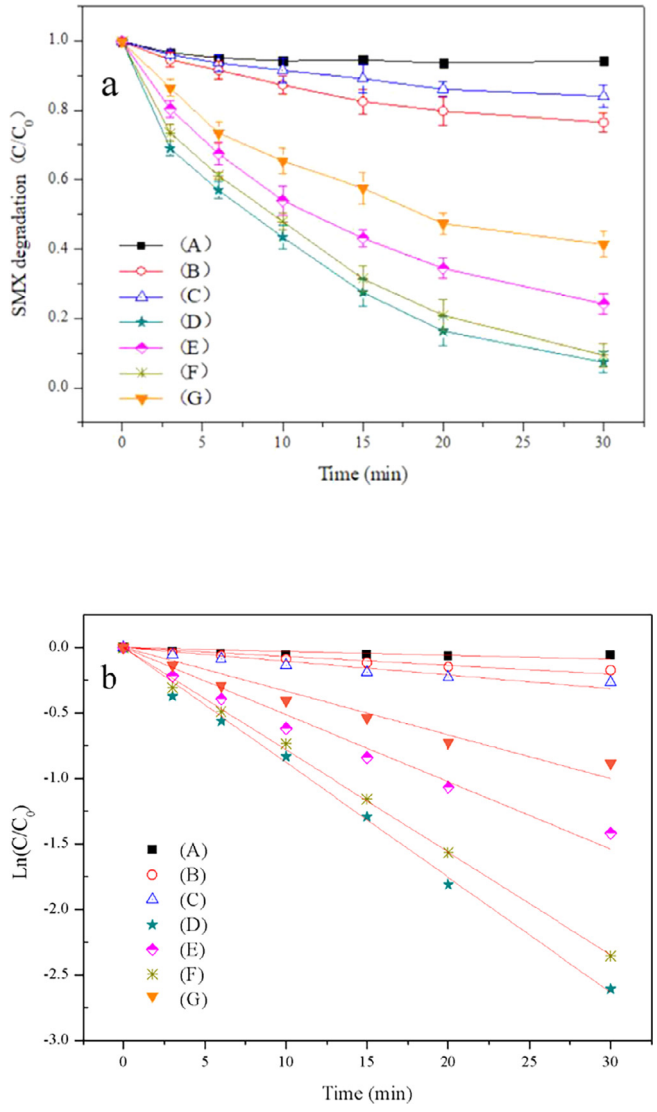

Fig. 2. (a) SMX degradation under different conditions and (b) the relative pseudo first order kinetic analysis results: (A) only Fe_3O_4/β-FeOOH, (B) only PMS, (C) Fe_3O_4 + PMS, (D) β-FeOOH + PMS, (E) physical mixture of Fe_3O_4 and β-FeOOH + PMS, (F) Fe_3O_4/β-FeOOH + PMS, (G) 0.0868 g/L β-FeOOH + PMS. (Reaction conditions: initial SMX concentration = 5 mg/L, catalyst dosage = 0.2 g/L, PMS dosage = 0.15 g/L, T = 298 K, pH = 7.5.)

through the facile one pot method.

3.2. High catalytic activity of Fe_3O_4/β-FeOOH for SMX degradation

The SMX degradation by Fe_3O_4/β-FeOOH activated PMS was evaluated without energy input. First, the degradation of SMX in PMS solution itself and PMS solution coupled with Fe_3O_4, β-FeOOH and Fe_3O_4/β-FeOOH were compared. As shown in Fig. 2, in the absence of PMS, about 5.7% reduction of SMX were detected after 30 min due to the adsorption effect of Fe_3O_4/β-FeOOH nanocomposites (curve A). Similarly, PMS can hardly oxidize SMX alone (curve B). In presence of PMS, about 22% of SMX was removed in 30 min with Fe3O4 nanoparticles (curve C), the β-FeOOH nanoparticles (curve D) induced the fastest SMX degradation efficiency to 94% in 30 min under the same condition. A mechanical mixture of Fe_3O_4 and β-FeOOH crystals with mole ratio of Fe_3O_4: β-FeOOH = 1:2 (curve E) was also used for comparison and induced SMX degradation efficiency to 75%. The addition of Fe_3O_4/β-FeOOH nanocomposites (curve F) increased SMX degradation with removal of 91% in 30 min under the same conditions. Moreover, the mass fraction of β-FeOOH in synthesized Fe_3O_4/β-FeOOH nanocomposites was about 43.4% (mole ratio of Fe_3O_4: β-FeOOH = 1:2). To clarify the exact role of Fe_3O_4 in the process of SMX degradation, 0.0868 g/L pure β-FeOOH nanoparticles (43.4% of 0.2 g/L) was added and 61% of SMX was removed after 30 min (curve G). It indicated that Fe_3O_4 in Fe_3O_4/β-FeOOH nanocomposites can promote SMX degradation. It can be seen that Fe_3O_4/β-FeOOH nanocomposites had nearly the same catalytic activity as β-FeOOH but can be separated much easier by external magnetic field. Therefore, the coupling of PMS with Fe_3O_4/β-FeOOH nanocomposites was used for SMX degradation in the sequent experiments. Besides, some reports about activation of PMS by Fe-containing catalyst to compare with β-FeOOH in this study was also listed in Table 1.

The SMX degradation in the Fe_3O_4/β-FeOOH/PMS system followed the pseudo-first order kinetics model ($R^2 > 0.95$), and the reaction constants (k_{obv}) for Fe3O4, β-FeOOH, 0.0868 g/L β-FeOOH, the physical mixture and Fe_3O_4/β-FeOOH was 0.0105 min^{-1}, 0.0878 min^{-1}, 0.0331 min^{-1}, 0.0513 min^{-1} and 0.0782 min^{-1} respectively. The results suggested that: a) the Fe(III) in β-FeOOH showed much higher catalytic activity in activation of PMS than that in Fe3O4, b) the Fe_3O_4/β-FeOOH nanocomposites synthesized via an energy saving route had great potential for PMS activation and c) there may be a synergistic mechanism on the surface of Fe_3O_4/β-FeOOH nanocomposites due to the interaction between β-FeOOH and Fe_3O_4.

Besides, the degradation pathway of SMX during PMS oxidation system has been investigated deeply in previous reports. So it need not be repeated here [36–38].

3.3. Effect of several operating parameters for SMX degradation in Fe_3O_4/β-FeOOH/PMS system

For meeting the requirement of practical application, some catalytic experiments were conducted to investigate the effects of several operating parameters on the SMX degradation.

3.3.1. Effect of catalyst dosage

The experiments of SMX degradation with different catalyst dosage were carried out. As shown in Fig. 3, a linear relationship ($R^2 = 0.96$) could be established between the k_{obv} and the Fe_3O_4/β-FeOOH dosage: $k_{obv} = 0.0253\ min^{-1} + m(Catalyst)_0 \times 0.203$ L/(gmin). The improvement of the reaction rate might be attribute to the increase of the active sites amount in solution [39], which may lead to more oxidants

Table 1
The activation of PMS by other heterogeneous Fe-containing catalysts.

catalyst	Reaction conditions							Degradation	Refs.
	Pollutant concentration	PMS concentration	Catalyst agent dose	Temperature °C)	pH	Reaction time	Assistant		
δ-FeOOH	50 mg/L	0.43 g/L	0.3 g/L	25	5.0	30 min	–	91.4%	[36]
Fe_3O_4	0.06 mM	3 mM	0.4 g/L	25	7.5	30 min	Ultrasound 0.2 kW	90%	[9]
α-Fe_2O_3	50 mg/L	1 mM	1.5 g/L	RT	7	60 min	–	95%	[46]
$CuFe_2O_4$	10 μmol/L	25 μM	0.04 g/L	25	7.0	15 min	–	100%	[37]
$Fe^{(0)}$	10 mg/L	0.2 mM	0.5 g/L	RT	7	30 min	–	95.2%	[38]

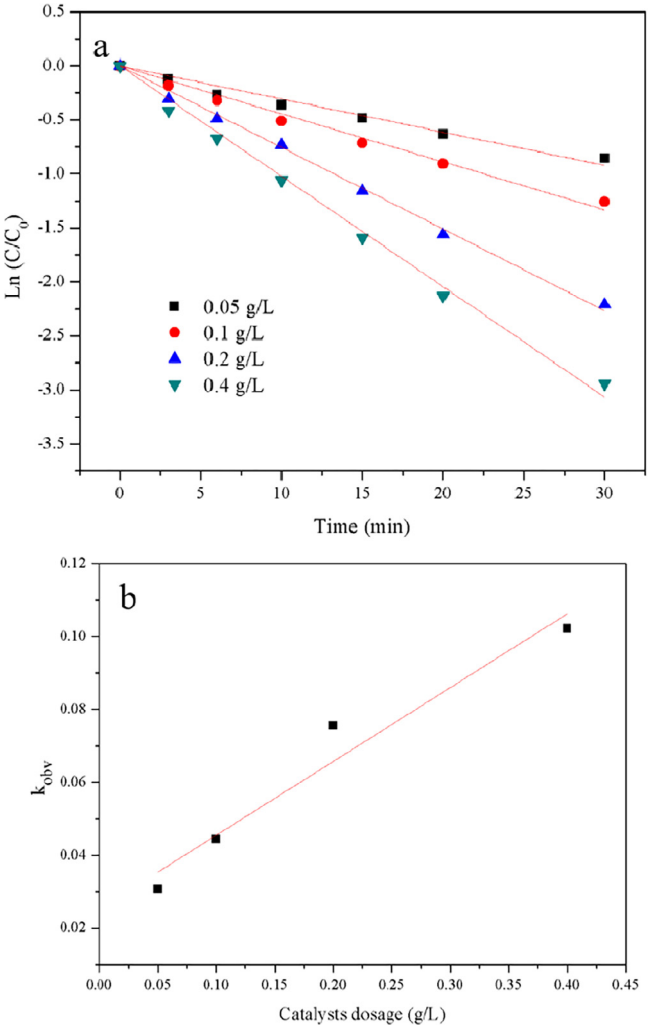

Fig. 3. Effect of catalyst dosage on SMX degradation: (a) The change of pseudo first order rate and (b) relation between catalyst dosage and pseudo first order rate. (Reaction conditions: initial SMX concentration = 5 mg/L, PMS dosage = 0.15 g/L, T = 298 K, pH = 7.5.)

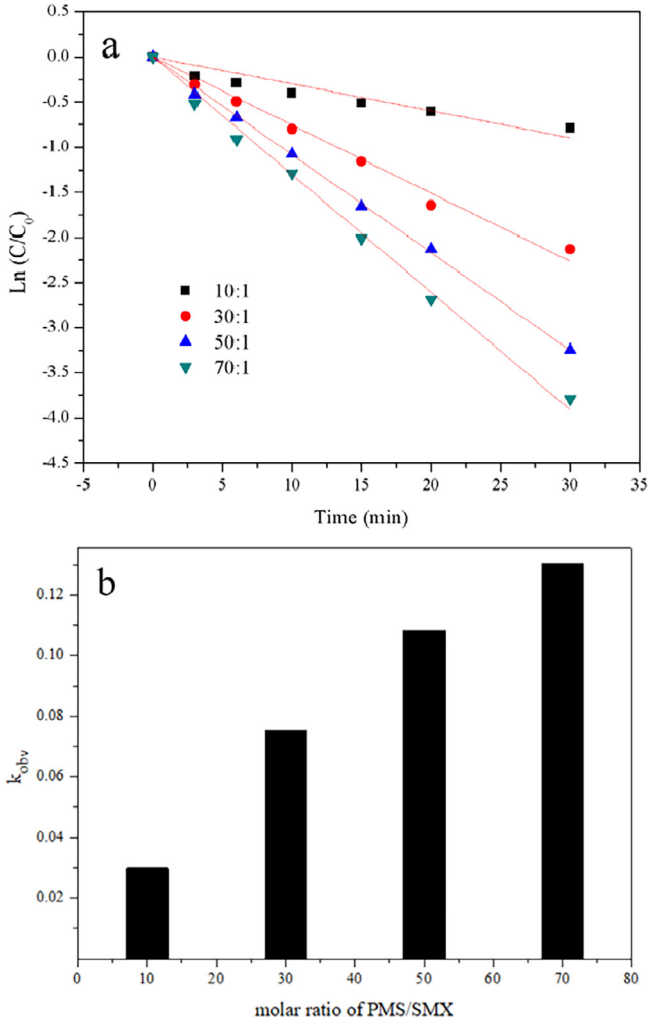

Fig. 4. Effect of PMS concentration on SMX degradation: (a) The change of pseudo first order rate and (b) k_{obv} at various PMS concentration. (Reaction conditions: initial SMX concentration = 5 mg/L, catalyst dosage = 0.2 g/L, T = 298 K, pH = 7.5.)

decompose in a given time, benefitting to the degradation of SMX.

3.3.2. Effect of PMS dosage

It can be seen from Fig. 4 that the SMX removal rate and k_{obv} at various PMS concentration. The removal efficiency of SMX increased with PMS concentration. When the molar ratio of PMS/SMX changed from 10:1 to 30:1, the k_{obv} of SMX degradation increased from 0.0298 min^{-1} to 0.0754 min^{-1}, then as the mole ratio of PMS/SMX increased from 30:1 to 70:1 the increasing rate of k_{obv} declined gradually. At low concentration of PMS, active sites on the catalyst surfaces could not be utilized effectively, the concentration of PMS was the rate limiting factor of the reaction. However, the usage of active sites tents to be saturated gradually with the increased concentration of PMS, which means at high concentration of PMS, the number of active sites on the catalyst surfaces was the limiting factor.

3.3.3. Effect of temperature

Temperature is one of the most important factors for activating PMS. Fig. 5a showed the degradation of SMX at different temperatures. The k_{obv} was 0.0868 min^{-1} at 298 K, while 0.126 min^{-1} at 308 K, then as the temperature increased to 328 K the degradation rate of SMX reached 0.322 min^{-1}. Additionally, the correlation between temperature and rate constant was further fitted with the Arrhenius equation (Fig. 5b, R2 = 0.96), the apparent activation energy was to be 37.41 kJ/mol. Considering the relationship between apparent activation energy and reaction types [40], the result suggested that the Fe_3O_4/β-FeOOH/PMS system was dominated by intrinsic chemical reaction. In addition, the apparent activation energy in Fe_3O_4/PMS-SMX system was 45.1 kJ mol^{-1} (Fig. S4), indicating that the catalytic activity of Fe_3O_4/β-FeOOH for SMX degradation was greater than that of Fe_3O_4.

3.3.4. Effect of pH

The change of solution pH on SMX degradation was studied. As shown in Fig. 6, the highest degradation of SMX was obtained under neutral condition, but the degradation rate decreased rapidly at acidic or alkaline condition. To avoid the influence of anions [41], solutions pH was buffered by sodium tetraborate instead of bicarbonate or hydrogen phosphate.

The solution pH showed great impact on Fe_3O_4/β–FeOOH/PMS system may be attributable to its effect to the surface charge of metal oxides and the fractions of different PMS species. The pH_{pzc} of Fe_3O_4 and β-FeOOH were 7.1 and 7.5, respectively [42], which means that the surface of catalyst was almost electroneutral under the neutral condition, and when the pH was higher or lower than pH_{pzc}, the catalyst surfaces was negatively or positively charged. On the other hand, pK_{a1} and pK_{a2} of PMS were 0 and 9.4, respectively [43]. Therefore, the dominant PMS species was HSO_5^- at condition of pH less than 9.4 and

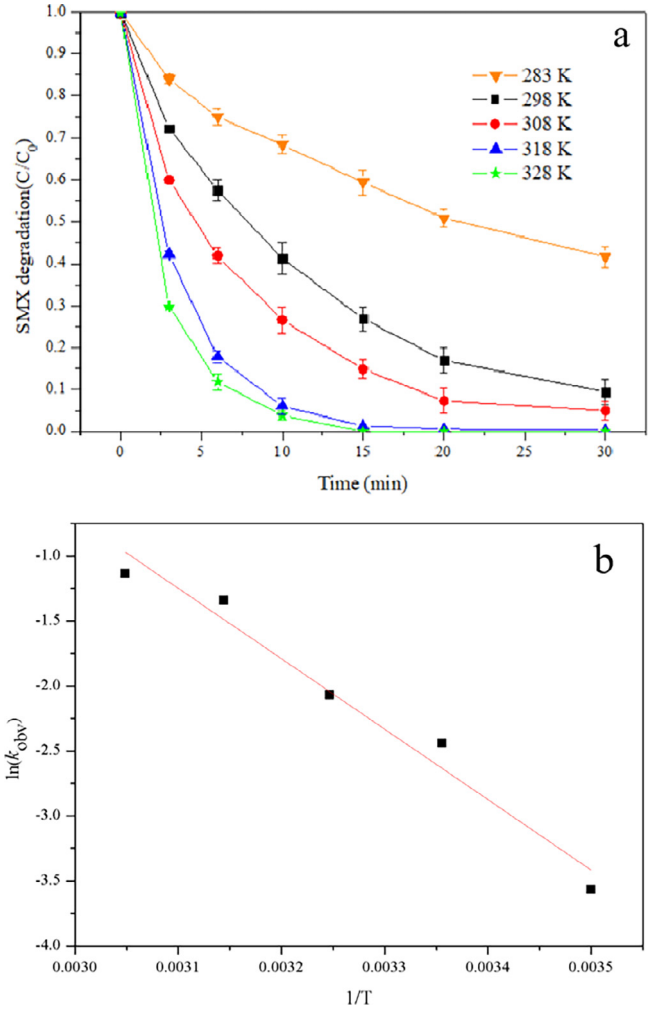

Fig. 5. Effect of temperature on SMX degradation: (a) SMX degradation under different temperatures and (b) Plot of ln(k_{obv}) versus 1/T in Fe_3O_4/β-FeOOH /PMS system. (Reaction conditions: initial SMX concentration = 5 mg/L, catalyst dosage = 0.2 g/L, PMS dosage = 0.15 g/L, pH = 7.5.)

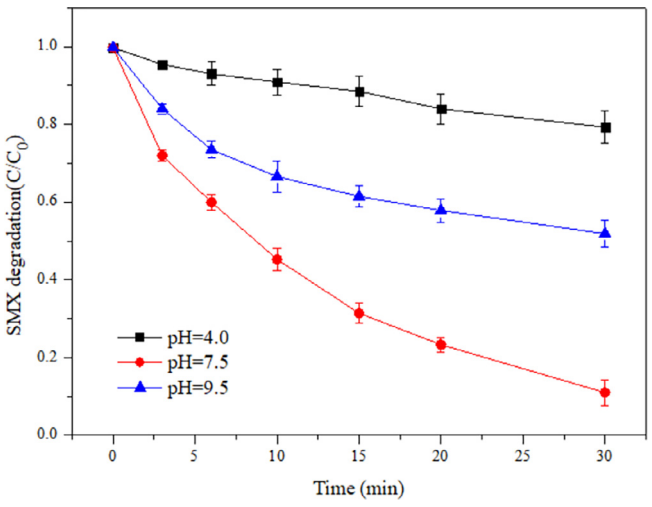

Fig.6. Effect of pH on SMX degradation. (Reaction conditions: initial SMX concentration = 5 mg/L, catalyst dosage = 0.2 g/L, PMS dosage = 0.15 g/L, T = 298 K.)

SO_5^{2-} at pH > 9.4. In acidic condition, the oxidant was difficult to be decomposed, more H-bond formed between H^+ and the O—O group of HSO_5^- which may hinder the reaction between positively charged catalyst surface and PMS. Moreover, $SO_4^{-\cdot}$ and ·OH could be scavenged by hydrogen ions according to Eqs. (1 and 2) [44,45], which was also responsible for the low degradation rate.

$$SO_4^{-\cdot} + H^+ + e^- \rightarrow HSO_4^{-\cdot} \quad (1)$$

$$OH^{\cdot} + H^+ + e^- \rightarrow H_2O \quad (2)$$

At pH = 9.5, electron repulsion reduced the interaction between SO_5^{2-} and negative charged surface. In addition, PMS can be self-decomposed through non-radical pathways and the leaching Fe ions can be deposited under the alkaline condition [46,47], which also reduced the degradation rate of SMX. Therefore, neutrality was the best reaction condition due to the weak repulsion between catalyst surface and HSO_5^-.

3.4. Metal leaching and reusability of Fe_3O_4/β-FeOOH

To evaluate the stability and reusability of Fe_3O_4/β-FeOOH nanocomposites, the SXM removal efficiency and the concentration of leached Fe ions were determined during successive catalytic experiments, the used catalysts were collected efficiently by magnetic separation and reused for five times. It can be seen from Fig. 7 that during the fifth test run, the SMX removal was about 81% in 30 min, decreased by only 10% compared with the first run. The TOC removal was decreased from 51% to 42% after the successive catalytic experiments (Fig. S5), demonstrating that Fe_3O_4/β-FeOOH possessed stable catalytic activity to activate PMS for SMX degradation. The concentration of leached Fe ions was determined as 0.29 mg L^{-1} in 30 min for the first run and stabilized on 0.51 mg L^{-1} during the fifth run, accounting for only 0.14–0.25% of total Fe content in the reaction system. The concentration of leached Fe ions at different pH levels was determined (Table 2), it can be seen that concentration of leached Fe after 30 min reaction increased significantly with the decrease of pH value, and even reach 0.76 mg/L at pH 3, which might lead to the homogeneous catalysis for PMS. Thus, the experiments of homogeneous catalysis were carried out to evaluate the contribution of leaching iron ions for SMX degradation. As shown in Fig. S6, only 23% and 20% of the SMX were removed in 30 min with 0.29 mg L^{-1} Fe^{2+} and Fe^{3+}. It indicated that Fe_3O_4/β-FeOOH had negligible influence on environment and the activation of PMS by Fe_3O_4/β-FeOOH was mainly through the heterogeneous way. In fact, although the composite catalyst will be lost by leaching under acidic conditions, its main purpose is to degrade pollutants in aqueous under neutral conditions. In neutral, the composite presented a strong chemical stability indeed. The excellent stability of recycled catalyst was further confirmed by XRD diffraction patterns (Fig. 8a), which showed no obvious changes of characteristic peaks compared with the fresh catalyst.

3.5. Possible active radical

·OH, $SO_4^{-\cdot}$, and $SO_5^{-\cdot}$ were commonly considered as three main possible types of reactive oxygen species (ROS) during the PMS activation process [14], the contribution of $SO_5^{-\cdot}$ for SMX degradation can be neglected considering its weak oxidizing ability [21]. To verify the dominating ROS present in the Fe_3O_4/β-FeOOH /PMS system, some quenching experiments were conducted. Ethanol and TBA were selected as quenching agents due to their different reaction rate with $SO_4^{-\cdot}$ and ·OH. The reaction rate of ethanol with $SO_4^{-\cdot}$ and ·OH are 1.6–7.7 × 10^9 mol/(L·s) and 1.2–2.8 × 10^9 mol/(L·s), respectively [9]. TBA can also easily react with ·OH (3.8–7.6 × 10^9 mol/(L·s)), but its reaction rate with $SO_4^{-\cdot}$ (4.0–9.1 × 10^5 mol/(L·s)) is much slower [17].Therefore, ethanol and TBA were used to distinguish $SO_4^{-\cdot}$ and ·OH. As shown in Fig. 9, the addition of 0.6 mol L^{-1} ethanol and TBA

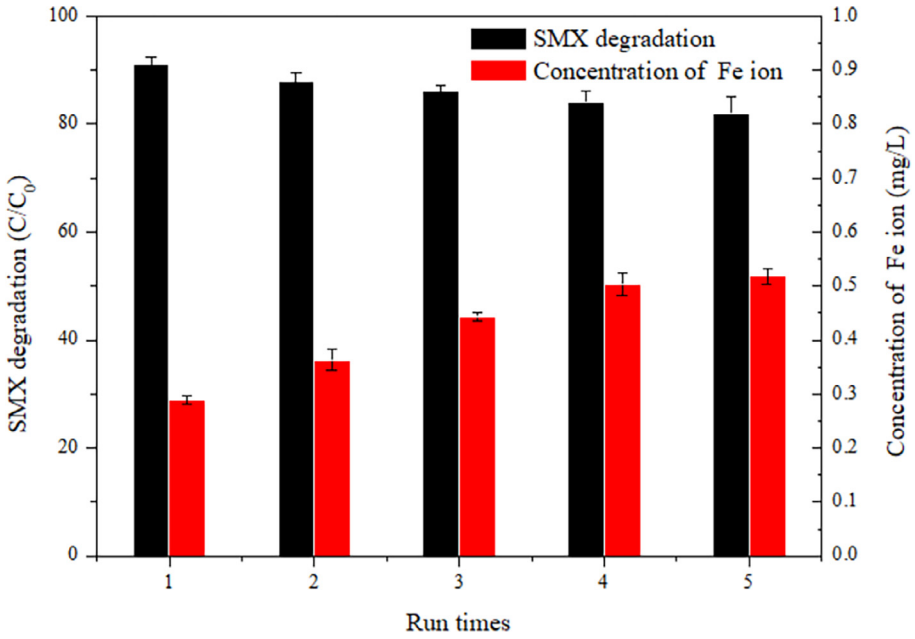

Fig. 7. Stability and reusability of Fe_3O_4/β-FeOOH to activate PMS for SMX degradation. (Reaction conditions: initial SMX concentration = 5 mg/L, catalyst dosage = 0.2 g/L, PMS dosage = 0.15 g/L, T = 298 K, pH = 7.5.)

Table 2
The concentration of leached Fe irons at different pH leaves after 30 min reaction.

pH	3	4	5	6	7	8	9
Leached Fe (mg/L)	0.76	0.54	0.38	0.32	0.29	0.25	0.24

(1000:1 M ratio of ethanol/TBA: PMS) decreased the SMX degradation efficiency from 91% to 60% and 83% in 30 min, respectively, which means both of ·OH and $SO_4^{-\cdot}$ were generated in the Fe_3O_4/β-FeOOH/PMS system while neither of them was the major oxidizing species. On the other hand, Na_2SO_3 can quench the oxidation processes completely, demonstrating that non-radical oxidation reaction may be responsible for the degradation of SMX. Thus, singlet oxygen ($^1O_2$) may be generated in the reaction with PMS and Fe_3O_4/β-FeOOH. Furfuryl alcohol (FFA) was reported to be the efficient quenchers for $^1O_2$ (1.2×10^8 mol/(L·s)) [48]. Fig. 9 showed that in the presence of FFA (0.6 mol L^{-1}), only 24% SMX was degraded, indicating the existence of $^1O_2$. It should be noted that FFA is also an efficient quencher for ·OH (1.5×10^{10} mol/(L·s)), if ·OH was the dominant ROS, TBA and FFA should have similar inhibitory effects. However, the comparison of the inhibitory effects of TBA (83%) and FFA (24%) indicated that $^1O_2$ was the dominant ROS at neutral conditions. In order to clarify the contributions of ROS at different pH, several quenching experiments were carried out at acidic and alkaline conditions (see Fig. S7). It was found that $SO_4^{-\cdot}$ and ·OH were the dominant ROS at pH = 4.0 while $^1O_2$ played the most important role at pH = 9.5. PMS activated via non-radical pathways showed best effect at neutral and alkaline conditions, the results were agreed with other studies [49,50].

To further confirm the generation of ROS in Fe_3O_4/β-FeOOH/PMS system, ESR studies were carried out using DMPO and TMP as spin trap agents. As shown in Fig. 10a, the typical peak in the spectra indicated that both DMPO-SO_4 and DMPO-OH existed [51], which agreed well with radical quenching tests. On the other hand, TMP can readily react with $^1O_2$ and be transformed into a stable radical TMPN [52]. In this study, a characteristic three-line EPR spectrum of TMPN (aN = 16.9 G, g = 2.0054) was observed in Fig. 10b, further indicating the existence of $^1O_2$ in Fe_3O_4/β-FeOOH/PMS system. Based on the above observations, it can be concluded that $SO_4^{-\cdot}$, ·OH and $^1O_2$ were generated

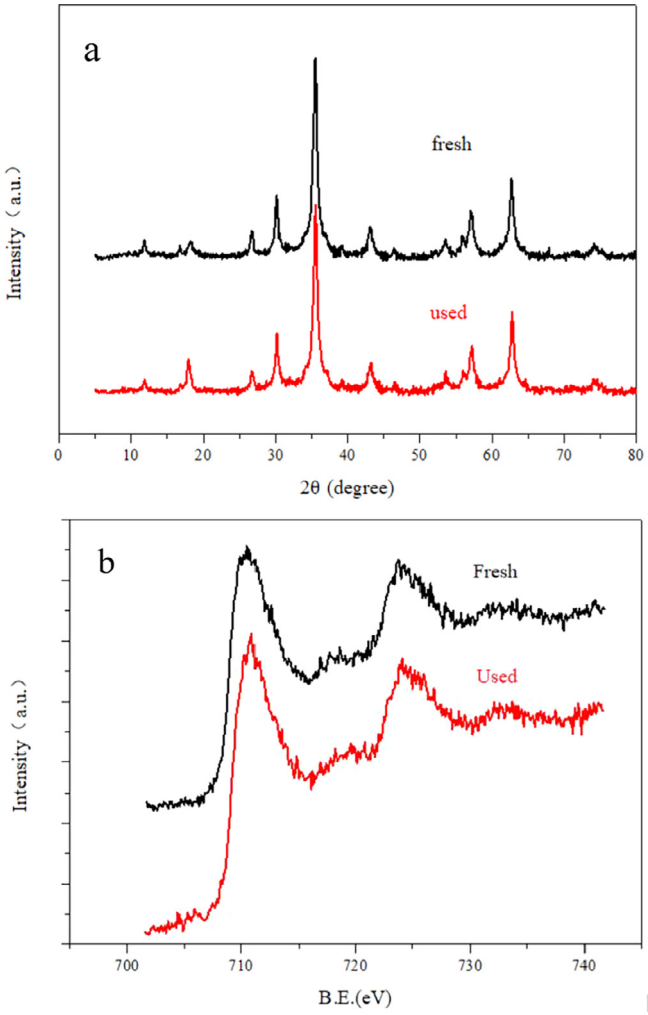

Fig. 8. (a) XRD pattern and (b) Fe 2p XPS spectrum of fresh and used Fe_3O_4/β-FeOOH nanocomposites.

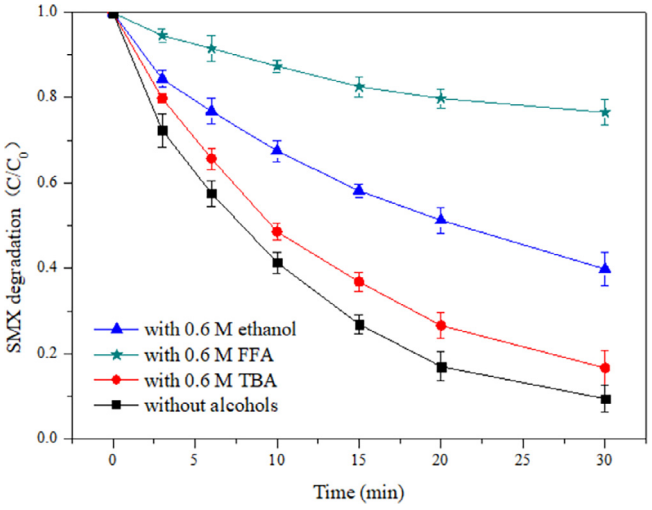

Fig. 9. Effect of radical scavengers on SMX degradation. (Reaction conditions: initial SMX concentration = 5 mg/L, catalyst dosage = 0.2 g/L, PMS dosage = 0.15 g/L, T = 298 K, pH = 7.5.)

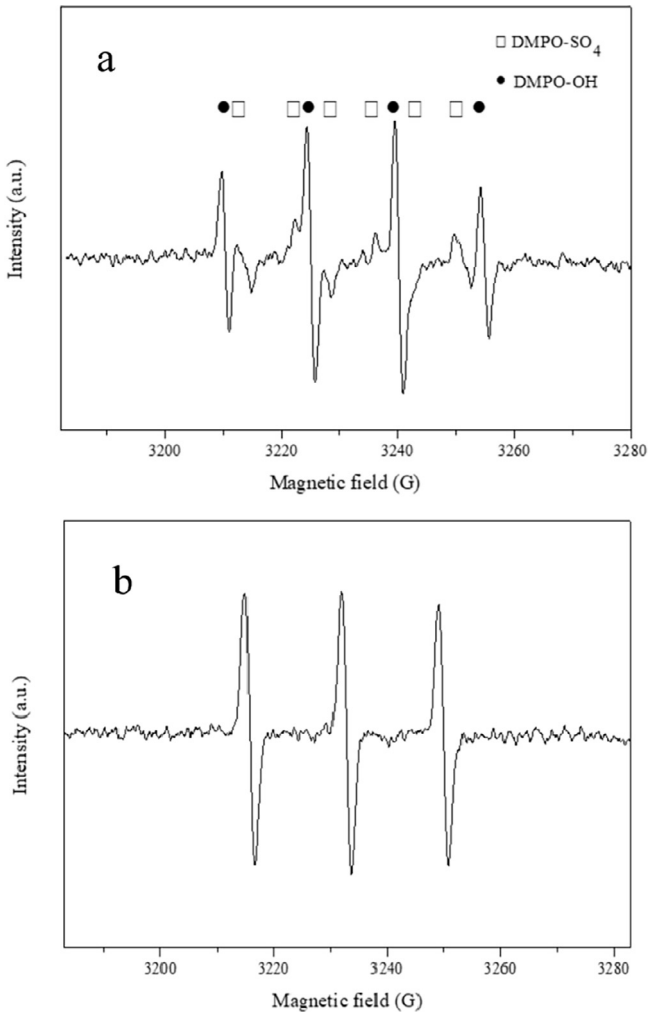

Fig. 10. ESR spectra in Fe_3O_4/β-FeOOH /PMS system using DMPO (a) and TMP (b) as spin-trapping agents. (Reaction conditions: catalyst dosage = 0.2 g/L, PMS dosage = 0.15 g/L, [DMPO] = [TMP] = 0.1 M, T = 298 K, pH = 7.5.)

during the reaction, $^1O_2$ was the dominant ROS responsible for the SMX degradation.

3.6. Possible mechanism of PMS activation by Fe_3O_4/β-FeOOH

It was believed that Fe(III)/Fe(II) on the Fe_3O_4/β-FeOOH surface played an important role on PMS activation. Thus, XPS was used to analyze the change of elements valence on catalyst surfaces before and after the reaction. Fig. 8b showed the Fe 2p XPS spectra of the fresh and used Fe_3O_4/β-FeOOH catalysts. The intense peak was observed at 710.5 eV for the fresh catalyst. After catalytic reactions, the Fe 2p3/2 binding energy was shifted positively from 710.5 to 710.9 eV, indicating that some Fe(II) on the catalyst surfaces was oxidized to Fe(III).

Finally, based on all the above experimental results obtained and previous researches, two different heterogeneous activation mechanisms of PMS by Fe_3O_4/β-FeOOH nanocomposites can be proposed.

The first was the conventional metal oxides catalytic process, which can react with PMS to produce radical species ($SO_4^{-\cdot}$, ·OH). According to experimental results and previous studies [53], Fe_3O_4 has a low catalytic activity for PMS. Therefore, the PMS would initially conjunct with the surface hydroxylated β-FeOOH and give one electron to catalyst to generate $SO_5^{-\cdot}$, while Fe(III) was transformed to Fe(II) (Eqs. (3 and 4)). On the other hands, PMS may also obtained one electron from catalysts to generate $SO_4^{-\cdot}$ and ·OH according to Eqs. (5–7), and Fe(II) was oxidized to Fe(III) at the same time. Considering the reaction rate of β-FeOOH/PMS and Fe_3O_4/PMS, electron density difference may exist on the interface between β-FeOOH and Fe_3O_4, which may induce local electron-transfer from Fe^{II}_{FeOOH} to $Fe^{III}_{Fe_3O_4}$ (Eq. (8)). In this way, the reaction of PMS and Fe_3O_4 was activated (Eqs. (9 and 10)). In addition, H_2O can react with $SO_4^{-\cdot}$ to produce ·OH (Eq. (11)). Finally, the SMX was degraded by $SO_4^{-\cdot}$ and ·OH (Eq. (12)).

$$\equiv Fe^{III}_{FeOOH}\text{–}OH + HSO_5^- \rightarrow \equiv Fe^{III}_{FeOOH}\text{–}(O)OSO_3^- + H_2O \quad (3)$$

$$\equiv Fe^{III}_{FeOOH}\text{–}(O)OSO_3^- + H_2O \rightarrow \equiv Fe^{II}_{FeOOH}\text{–}OH + SO_5^{-\cdot} + H^+ \quad (4)$$

$$\equiv Fe^{II}_{FeOOH}\text{–}OH + HSO_5^- \rightarrow \equiv Fe^{II}_{FeOOH}\text{–}(O)OSO_3^- + H_2O \quad (5)$$

$$\equiv Fe^{II}_{FeOOH}\text{–}(O)OSO_3^- + H_2O \rightarrow \equiv Fe^{III}_{FeOOH}\text{–}OH + SO_4^{-\cdot} + OH^- \quad (6)$$

$$\equiv Fe^{II}_{FeOOH}\text{–}(O)OSO_3^- + H_2O \rightarrow \equiv Fe^{III}_{FeOOH}\text{–}OH + SO_4^{2-} + \cdot OH \quad (7)$$

$$\equiv Fe^{II}_{FeOOH}\text{–}OH + \equiv Fe^{III}_{Fe_3O_4}\text{–}OH \rightarrow \equiv Fe^{III}_{FeOOH}\text{–}OH + \equiv Fe^{II}_{Fe_3O_4}\text{–}OH \quad (8)$$

$$\equiv Fe^{II}_{Fe_3O_4}\text{–}OH + HSO_5^- \rightarrow \equiv Fe^{II}_{Fe_3O_4}\text{–}(O)OSO_3^- + H_2O \quad (9)$$

$$\equiv Fe^{II}_{Fe_3O_4}\text{–}(O)OSO_3^- + H_2O \rightarrow \equiv Fe^{III}_{Fe_3O_4}\text{–}OH + SO_4^{-\cdot} + OH^- \quad (10)$$

$$SO_4^{-\cdot} + H_2O \rightarrow \cdot OH + H^+ + SO_4^{2-} \quad (11)$$

$$SMX + SO_4^{-\cdot}/\cdot OH \rightarrow \text{intermediate} \rightarrow CO_2 + H_2O \quad (12)$$

The second was non-radical oxidation process, which can decompose PMS with the generation of $^1O_2$. Generally, $^1O_2$ can be produced from PMS activation catalyzed by carbon catalysts and noble metal or copper doped materials. Ma et al. synthesized ZIF-67 derived nitrogen-doped carbon nanotubes frameworks (NCNTFs) to degrade bisphenol A (BPA) in presence of PMS and found that $^1O_2$ was dominated in the degradation of BPA. The nitrogen-doped carbon nanotubes could enhance the nonradical pathway by facilitating electron transfer [54]. Wang et al. used Pd/g-C3N4 to degrade bisphenol A (BPA) with PMS and demonstrated that the major ROS was also $^1O_2$. The novel metal Pd can help PMS to accept electrons from BPA directly and it is believed that the anchored Pd in catalyst was the key factor for $^1O_2$ generation [12]. In a word, these materials can serve as electron transfer mediators due to the excellent conductivity [55]. However, β-FeOOH has poor conductivity, so the non-radical mechanism in Fe_3O_4/β-FeOOH/PMS system may be different from previous studies. In recent studies,

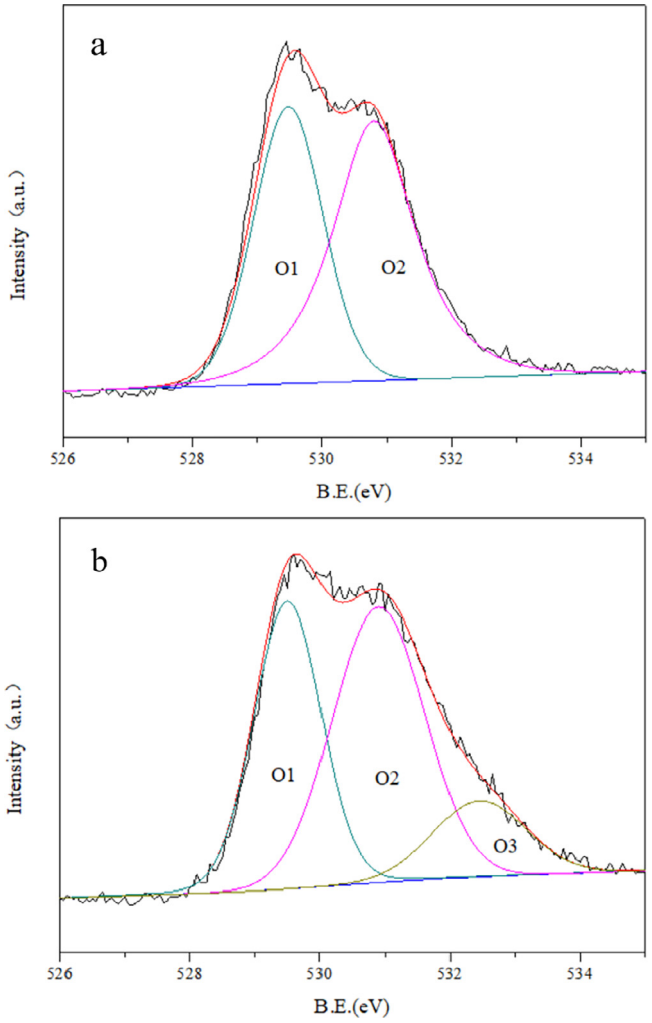

Fig. 11. O 1 s XPS spectrum of Fe_3O_4/β-FeOOH nanocomposites before and after SMX degradation reaction.

nanoscale β-FeOOH were found to have excellent catalytic activity in oxygen evolution reaction (OER) probably due to the special tunnel-type structure and abundant oxygen vacancies on the surface, which could provide more active sites [56,57]. It can be speculated that the oxygen vacancies may also be responsible for the non-radical oxidation process. To better understand the non-radical oxidation process, the O 1 s XPS spectra of Fe_3O_4/β-FeOOH before and after degradation reaction were analyzed. As shown in Fig. 11, O1 and O2 were identified by peaks at 529.5 eV and 530.9 eV before the reaction. In comparison, a new peak at 532.4 eV indicated the existence of O3 after the catalyst reaction. O(1) was corresponded to lattice oxygen, O2 was associated with defect sites (oxygen vacancies) with low oxygen coordination and O3 was attributed to physically adsorbed oxygen [57,58]. It can be seen that the atomic percentages of lattice oxygen (O1) was down to 37.9% from 44.8% after SMX degradation experiments. The result confirmed that the generated $^1O_2$ in Fe_3O_4/β-FeOOH/PMS system come from lattice oxygen. During the reaction, some lattice oxygen atoms (O_{lat}) could be released with the generation of oxygen vacancies and then transformed into active oxygen (O^*), which could react with PMS and convert to $^1O_2$ (Eqs. (13 and 14)) [59]. On the other hands, the presence of oxygen vacancies can also activate chemisorbed oxygen to form $^1O_2$ [60]. In addition, a small fraction of $^1O_2$ could be generated from the self-decomposition of PMS (Eq. (15)) [39].

$$O_{lat} \rightarrow O^* \quad (13)$$

$$O^* + HSO_5^- \rightarrow HSO_4^- + 1\,O_2 \quad (14)$$

$$SO_5^{2-} + HSO_5^- \rightarrow HSO_4^- + SO_4^{2-} + 1\,O_2 \quad (15)$$

According to the results, special tunnel-type structure (Fig. 12) and other papers, several characteristics of nanoscale β-FeOOH may be beneficial for PMS activation during the catalytic reaction process: (a) the excellent adsorption ability for inorganic anions and pollutants due to high specific surface area and hydrogen bonding [61], which can accelerate the reaction by increasing local reactants concentration; (b) abundant hydroxyl groups on catalyst surfaces caused by the central Cl ion in the tunnel-type structure [56], which plays a key role in the process of PMS activation [62]; (c) abundant oxygen vacancies on catalyst surfaces due to the acidic condition when synthesis [63], which participates in the generation of $^1O_2$.

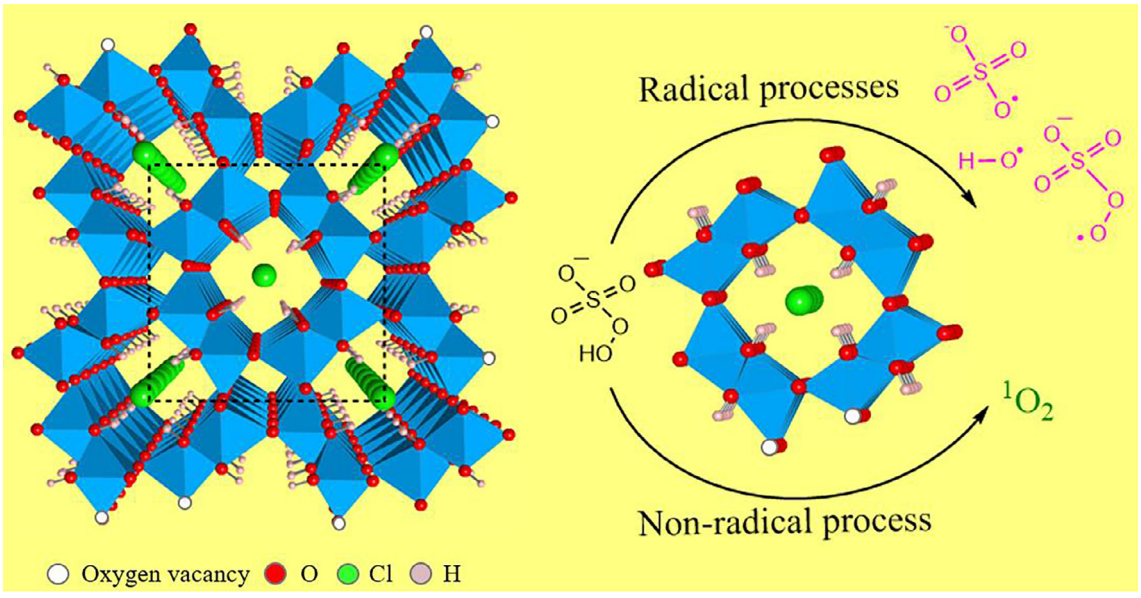

Fig. 12. Cl ions supported tunnel-type structure of β-FeOOH.

4. Conclusions

In this study, the environmental friendly magnetic Fe_3O_4/β-FeOOH nanocomposites with low-cost were prepared via a facile one pot method, which exhibited excellent catalytic activity towards PMS to degrade SMX under the experimental conditions. Under neutral condition, by using 0.2 g L^{-1} Fe_3O_4/β-FeOOH nanoparticles and 0.15 g L^{-1} PMS, 91% of SMX (5 mg L^{-1}) was degraded in 30 min. The catalyst showed the great stability and reusability during the successive repeated reactions. According to quenching tests and ESR analysis, $SO_4^{-\cdot}$, ·OH and $^1O_2$ were generated in PMS-Fe_3O_4/β-FeOOH system, and the main species were $SO_4^{-\cdot}$ and $^1O_2$. Fe_3O_4/β-FeOOH could degrade SMX by activating PMS in both radical and non-radical oxidation process, this may thank to the unique tunnel-type structure and surface oxygen vacancies.

Acknowledgment

This work was supported by the National Natural Science Foundation of China (Grant No. 51508564).

Appendix A. Supplementary data

Supplementary data associated with this article can be found, in the online version, at https://doi.org/10.1016/j.cej.2018.09.064.

References

[1] M. Magureanu, D. Piroi, N.B. Mandache, V. David, A. Medvedovici, C. Bradu, V.I. Parvulescu, Degradation of antibiotics in water by non-thermal plasma treatment, Water Res. 45 (2011) 3407–3416.
[2] Y. Ji, C. Ferronato, A. Salvador, X. Yang, J.M. Chovelon, Degradation of ciprofloxacin and sulfamethoxazole by ferrous-activated persulfate: implications for remediation of groundwater contaminated by antibiotics, Sci. Total Environ. 472 (2014) 800–808.
[3] M. Długosz, P. Żmudzki, A. Kwiecień, K. Szczubiałka, J. Krzek, M. Nowakowska, Photocatalytic degradation of sulfamethoxazole in aqueous solution using a floating TiO_2-expanded perlite photocatalyst, J. Hazard. Mater. 298 (2015) 146.
[4] W. Baran, J. Sochacka, W. Wardas, Toxicity and biodegradability of sulfonamides and products of their photocatalytic degradation in aqueous solutions, Chemosphere. 65 (2006) 1295–1299.
[5] T. An, H. Yang, G. Li, W. Song, W.J. Cooper, X.P. Nie, Kinetics and mechanism of advanced oxidation processes (AOPs) in degradation of ciprofloxacin in water, Appl. Catal. B-Environ. 94 (2010) 288–294.
[6] W.D. Oh, Z. Dong, G. Ronn, T.T. Lim, Surface–active bismuth ferrite as superior peroxymonosulfate activator for aqueous sulfamethoxazole removal: Performance, mechanism and quantification of sulfate radical, J. Hazard. Mater. 325 (2016) 71–81.
[7] J. Liu, Z.W. Zhao, P.H. Shao, F.Y. Cui, Activation of peroxymonosulfate with magnetic Fe_3O_4–MnO_2 core–shell nanocomposites for 4-chlorophenol degradation, Chem. Eng. J. 262 (2015) 854–861.
[8] X. Ao, W. Liu, Degradation of sulfamethoxazole by medium pressure UV and oxidants: peroxymonosulfate, persulfate, and hydrogen peroxide, Chem. Eng. J. 313 (2017) 629–637.
[9] J. Liu, J. Zhou, Z. Ding, Z. Zhao, X. Xu, Z. Fang, Ultrasound irritation enhanced heterogeneous activation of peroxymonosulfate with Fe_3O_4 for degradation of azo dye, Ultrason. Sonochem. 34 (2017) 953–959.
[10] F. Ghanbari, F. Moradi, Application of peroxymonosulfate and its activation methods for degradation of environmental organic pollutants: Review, Chem. Eng. J. 102 (2017) 307–315.
[11] J. Hou, S. Yang, H. Wan, H. Fu, X. Qu, Z. Xu, S. Zheng, Highly effective catalytic peroxymonosulfate activation on N-doped mesoporous carbon for *o*-phenylphenol degradation, Chemosphere 197 (2018) 485–493.
[12] Y. Wang, D. Cao, M. Liu, X. Zhao, Insights into heterogeneous catalytic activation of peroxymonosulfate by Pd/g-C_3N_4: The role of superoxide radical and singlet oxygen, Catal. Commun. 102 (2017) 85–88.
[13] S. Wacławek, H.V. Lutze, K. Grübel, V. Padil, M. Černík, D.D. Dionysiou, Chemistry of persulfates in water and wastewater treatment: a review, Chem. Eng. J. 330 (2017) 44–62.
[14] G.P. Anipsitakis, D.D. Dionysiou, Radical generation by the interaction of transition metals with common oxidants, Environ. Sci. Technol. 38 (2004) 3705–3712.
[15] F. Qi, W. Chu, B. Xu, Catalytic degradation of caffeine in aqueous solutions by cobalt-MCM41 activation of peroxymonosulfate, Appl. Catal. B-Environ. 134 (2013) 324–332.
[16] K. Lin, H. Chang, Zeolitic imidazole framework-67 (ZIF-67) as a heterogeneous catalyst to activate peroxymonosulfate for degradation of Rhodamine B in water, J. Taiwan. Inst. Chem. E. 53 (2015) 40–45.
[17] T. Zeng, X. Zhang, S. Wang, H. Niu, Y. Cai, Spatial confinement of a Co_3O_4 catalyst in hollow metal-organic frameworks as a nanoreactor for improved degradation of organic pollutants, Environ. Sci. Technol. 49 (2015) 2350–2357.
[18] H. Sun, G. Zhou, S. Liu, H.M. Ang, M.O. Tade, S. Wang, Nano-Fe^0 encapsulated in micro-carbon spheres: synthesis, characterization, and environmental applications, ACS Appl. Mater. Interface. 4 (2012) 6235–6241.
[19] F. Gong, L. Wang, D. Li, F. Zhou, Y. Yao, W. Lu, S. Huang, W. Chen, An effective heterogeneous iron-based catalyst to activate peroxymonosulfate for organic contaminants removal, Chem. Eng. J. 267 (2015) 102–110.
[20] Y. Ding, L. Zhu, N. Wang, H. Tang, Sulfate radicals induced degradation of tetrabromo-bisphenol A with nanoscaled magnetic $CuFe_2O_4$ as a heterogeneous catalyst of peroxymonosulfate, Appl. Catal. B-Environ. 129 (2013) 153–162.
[21] Y. Ding, H. Tang, S. Zhang, S. Wang, H. Tang, Efficient degradation of carbamazepine by easily recyclable microscaled $CuFeO_2$ mediated heterogeneous activation of peroxymonosulfate, J. Hazard. Mater. 317 (2016) 686–694.
[22] J. He, W. Ma, W. Song, J. Zhao, X. Qian, Photoreaction of aromatic compounds at alpha-FeOOH/H_2O interface in the presence of H_2O_2: evidence for organic-goethite surface complex formation, Water Res. 39 (2005) 119–128.
[23] M. Muruganandham, A.J. Yang, J.J. Wu, Effect of ultrasonic irradiation on the catalytic activity and stability of goethite catalyst in the presence of H_2O_2 at acidic medium, Ind. Eng. Chem. Res. 46 (2017) 691–698.
[24] X. Qian, M. Ren, Y. Zhu, D. Yue, Y. Han, J. Jia, Y. Zhao, Visible light assisted heterogeneous Fenton-like degradation of organic pollutant via α-FeOOH/mesoporous carbon composites, Environ. Sci. Technol. 51 (2017) 3993–4000.
[25] G. Nie, J. Huang, Y. Hu, Y. Ding, X. Han, H. Tang, Heterogeneous catalytic activation of peroxymonosulfate for efficient degradation of organic pollutants by magnetic Cu^0/Fe_3O_4 submicron composites, Chinese J. Catal. 38 (2017) 227–239.
[26] M.A. Zazouli, F. Ghanbari, M. Yousefi, S. Madihi-Bidgoli, Photocatalytic degradation of food dye by Fe_3O_4–TiO_2 nanoparticles in presence of peroxymonosulfate: The effect of UV sources, J. Environ. Chem. Eng. 5 (2017) 2459–2468.
[27] A. Kumar, S.K. Gupta, Synthesis of adenine mediated superparamagnetic colloidal β-FeOOH nanostructure(s): study of their morphological changes and magnetic behavior, J. Nanopart. Res. 15 (2013) 1466.
[28] H. Jin, X. Tian, Y. Nie, Z. Zhou, C. Yang, Y. Li, L. Lu, Oxygen vacancy promoted heterogeneous Fenton-like degradation of Ofloxacin at pH 3.2-9.0 by Cu substituted magnetic Fe_3O_4@FeOOH nanocomposite, Environ. Sci. Technol. 51 (2017) 12699–12706.
[29] T. Yamashita, P. Hayes, Analysis of XPS spectra of Fe^{2+} and Fe^{3+} ions in oxide materials, Appl. Surf. Sci. 254 (2008) 2441–2449.
[30] L. Feng, M. Cao, X. Ma, Y. Zhu, C. Hu, Superparamagnetic high-surface-area Fe_3O_4, nanoparticles as adsorbents for arsenic removal, J. Hazard. Mater. 217–218 (2012) 439–446.
[31] J. Mohapatra, A. Mitra, D. Bahadur, M. Aslam, Surface controlled synthesis of MFe2O4 (m= Mn, Fe Co, Ni and Zn) nanoparticles and their magnetic characteristics, Crystengcomm 15 (2012) 524–532.
[32] Z. Qi, T.P. Joshi, R. Liu, H. Liu, J. Qu, Synthesis of Ce(III)-doped Fe_3O_4 magnetic particles for efficient removal of antimony from aqueous solution, J. Hazard. Mater. 329 (2017) 193–204.
[33] S. Nasrazadani, A. Raman, The application of infrared spectroscopy to the study of rust systems—II. Study of cation deficiency in magnetite (Fe_3O_4) produced during its transformation to maghemite (γ-Fe_2O_3) and hematite (α-Fe_2O_3), Corros. Sci. 34 (1993) 1355–1365.
[34] S. Potter, Economically viable synthesis of Fe_3O_4 nanoparticles and their characterization, Pol. J. Chem. Technol. 13 (2011) 1–5.
[35] N. Jaafarzadeh, F. Ghanbari, M. Ahmadi, Catalytic degradation of 2,4-dichlorophenoxyacetic acid (2,4-D) by nano-Fe_2O_3 activated peroxymonosulfate: Influential factors and mechanism determination, Chemosphere 169 (2016) 568.
[36] J. Fan, Z. Zhao, Z. Ding, J. Liu, Synthesis of different crystallographic FeOOH catalysts for peroxymonosulfate activation towards organic matter degradation, Rsc Advances 8 (2018) 7269–7279.
[37] D. Miao, J. Peng, M. Wang, S. Shao, L. Wang, S. Gao, Removal of atorvastatin in water mediated by $CuFe_2O_4$ activated peroxymonosulfate, Chemical Engineering Journal 346 (2018).
[38] C. Tan, Y. Dong, D. Fu, N. Gao, J. Ma, X. Liu, Chloramphenicol removal by zero valent iron activated peroxymonosulfate system: Kinetics and mechanism of radical generation, Chemical Engineering Journal 334 (2017).
[39] C. Tan, N. Gao, D. Fu, J. Deng, L. Deng, Efficient degradation of paracetamol with nanoscaled magnetic $CoFe_2O_4$ and $MnFe_2O_4$ as a heterogeneous catalyst of peroxymonosulfate, Sep. Purif. Technol. 175 (2017) 47–57.
[40] Y. Feng, D. Wu, Y. Deng, T. Zhang, K. Shih, Sulfate radical-mediated degradation of sulfadiazine by $CuFeO_2$ rhombohedral crystal-catalyzed peroxymonosulfate: synergistic effects and mechanisms, Environ. Sci. Technol. 50 (2016) 3119–3127.
[41] Y. Yao, H. Chen, J. Qin, G. Wu, C. Lian, J. Zhang, S. Wang, Iron encapsulated in boron and nitrogen codoped carbon nanotubes as synergistic catalysts for Fenton-like reaction, Water Res. 101 (2016) 281–291.
[42] K.M. Parida, Effect of Anions (Cl^-, SO_4^{2-}) on the Interfacial Properties of akaganeite (β-FeOOH) in aqueous electrolyte solutions, Adsorpt. Sci. Technol. 5 (1988) 257–279.
[43] Y. Ren, L. Lin, J. Ma, J. Yang, J. Feng, Z. Fan, Sulfate radicals induced from peroxymonosulfate by magnetic ferrospinel MFe_2O_4 (M = Fe Co, Cu, Mn, and Zn) as heterogeneous catalysts in the water, Appl. Catal. B-Environ. 165 (2015) 572–578.
[44] Y.H. Huang, Y.F. Huang, C.I. Huang, C.Y. Chen, Efficient decolorization of azo dye reactive black b involving aromatic fragment degradation in buffered Co^{2+}/pms oxidative processes with a ppb level dosage of co^{2+}-catalyst, J. Hazard. Mater. 170 (2009) 1110–1118.
[45] M. Ahmadi, F. Ghanbari, Combination of UVC-LEDs and ultrasound for

peroxymonosulfate activation to degrade synthetic dye: influence of promotional and inhibitory agents and application for real wastewater, Environ. Sci. Pollut. R. 25 (2018) 6003–6014.
[46] F. Ji, C. Li, X. Wei, J. Yu, Efficient performance of porous Fe_2O_3 in heterogeneous activation of peroxymonosulfate for decolorization of Rhodamine B, Chem. Eng. J. 231 (2013) 434–440.
[47] A. Rastogi, S.R. Al-Abed, D.D. Dionysiou, Sulfate radical-based ferrous-peroxymonosulfate oxidative system for PCBs degradation in aqueous and sediment systems, Appl. Catal. B-Environ. 85 (2009) 171–179.
[48] Y. Zhou, J. Jiang, Y. Gao, J. Ma, S.Y. Pang, J. Li, X. Lu, L. Yuan, Activation of Peroxymonosulfate by Benzoquinone: A novel nonradical oxidation process, Environ. Sci. Technol. 49 (2015) 12941–12950.
[49] W. Peng, J. Liu, C. Li, F. Zong, W. Xu, X. Zhang, Z. Fang, A multipath peroxymonosulfate activation process over supported by magnetic CuO-Fe_3O_4, nanoparticles for efficient degradation of 4-chlorophenol.“ Korean, Chem. Eng. J. (2018) 1–11.
[50] X. Duan, H. Sun, M. Tade, S. Wang, Metal-free activation of persulfate by cubic mesoporous carbons for catalytic oxidation via radical and nonradical processes, Catal. Today 307 (2017) 141–146.
[51] Y. Wang, H. Sun, H.M. Ang, M.O. Tadé, S. Wang, 3D-hierarchically structured MnO_2 for catalytic oxidation of phenol solutions by activation of peroxymonosulfate: Structure dependence and mechanism, Appl. Catal. B-Environ. 164 (2015) 159–167.
[52] Y. Zhou, J. Jiang, Y. Gao, S. Pang, Y. Yang, J. Ma, J. Gu, J. Li, Z. Wang, L. Wang, L. Yuan, Y. Yang, Activation of peroxymonosulfate by phenols: Important role of quinone intermediates and involvement of singlet oxygen, Water Res. 125 (2017) 209–218.
[53] C. Tan, N. Gao, Y. Deng, J. Deng, S. Zhou, J. Li, X. Xin, Radical induced degradation of acetaminophen with Fe_3O_4 magnetic nanoparticles as heterogeneous activator of peroxymonosulfate, J. Hazard. Mater. 276 (2014) 452–460.
[54] W. Ma, N. Wang, Y. Fan, T. Tong, X. Han, Y. Du, Non-radical-dominated catalytic degradation of bisphenol A by ZIF-67 derived nitrogen-doped carbon nanotubes frameworks in the presence of peroxymonosulfate, Chem. Eng. J. 336 (2018) 721–731.
[55] X. Cheng, H. Guo, Y. Zhang, X. Wu, Y. Liu, Non-photochemical production of singlet oxygen via activation of persulfate by carbon nanotubes, Water Res. 113 (2017) 80–88.
[56] T.M. Suzuki, T. Nonaka, A. Suda, N. Suzuki, Y. Matsuoka, T. Arai, S. Sato, T. Morikawa, Highly crystalline β-FeOOH(Cl) nanorod catalysts doped with transition metals for efficient water oxidation, Sustain. Energ. Fuel. 1 (2017) 636–643.
[57] Y. Bi, B. Zhang, L. Wang, Y. Zhang, Y. Ding, Ultrathin FeOOH Nanolayers with abundant oxygen vacancies on $BiVO_4$ photoanodes for efficient water oxidation, Angew. Chem. Int. Edit. 57 (2018) 2248–2252.
[58] Y. Ding, G. Zhang, X. Wang, L. Zhu, H. Tang, Chemical and photocatalytic oxidative degradation of carbamazepine by using metastable Bi^{3+} self-doped $NaBiO_3$ nanosheets as a bifunctional material, Appl. Catal. B-Environ. 202 (2017) 528–538.
[59] Y. Liu, H. Guo, Y. Zhang, W. Tang, X. Cheng, W. Li, Heterogeneous activation of peroxymonosulfate by sillenite $Bi_{25}FeO_{40}$: Singlet oxygen generation and degradation for aquatic levofloxacin, Chem. Eng. J. 343 (2018) 128–137.
[60] Y. Hao, B. Liu, L. Tian, F. Li, J. Ren, S. Liu, Y. Liu, J. Zhao, X. Wang, Synthesis of 111 facet-exposed MgO with surface oxygen vacancies for reactive oxygen species generation in the dark, ACS Appl. Mater. Interface. 9 (2017) 12687–12693.
[61] H. Morimoto, K. Takeno, Y. Uozumi, K. Sugimoto, S. Tobishima, High-rate charge-discharge performances of β-feooh-carbon composite electrodes, Key Eng. Mater. 301 (2006) 139–142.
[62] W.D. Oh, Z. Dong, T.T. Lim, Generation of sulfate radical through heterogeneous catalysis for organic contaminants removal: Current development, challenges and prospects, Appl. Catal. B-Environ. 194 (2016) 169–201.
[63] T. Zhang, Y. Ding, H Tang Generation of singlet oxygen over Bi(V)/Bi(III) composite and its use for oxidative degradation of organic pollutants, Chem. Eng. J. 264 (2015) 681–689.